

Article

# Hydrodynamic Conjunction of Textured Journal Surface—Bearing for Improved Frictional Response during Warm-Up of an Internal Combustion Engine

Ali Usman <sup>1</sup>, Sadia Riaz <sup>2</sup> and Cheol Woo Park <sup>3,\*</sup> 

<sup>1</sup> Department of Mechanical Engineering, COMSATS University Islamabad, Wah Cantt 47040, Pakistan; drusman@ciitwah.edu.pk

<sup>2</sup> Department of Mechanical Engineering, NUST College of EME, National University of Sciences and Technology, Islamabad 44000, Pakistan; sadia.riaz123@ceme.nust.edu.pk

<sup>3</sup> School of Mechanical Engineering, Kyungpook National University, Daegu 701-702, Korea

\* Correspondence: chwoopark@knu.ac.kr; Tel.: +82-53-950-7569; Fax: +82-53-950-6550

Received: 9 November 2018; Accepted: 11 December 2018; Published: 17 December 2018



**Abstract:** Considerable prime global energy is used in the transport sector. Significant energy is lost to overcome the internal friction of engines in transport vehicles. Journal bearings are crucial tribo-pairs and passive components that cause energy loss. Frictional losses increase extensively during the warm-up period of an engine due to high lubricant viscosity. Recent tribological developments have shown that surface textures can be a potential solution to reduce friction. A numerical investigation is performed to evaluate the effect of surface texture on the frictional and lubrication performance of a journal bearing at varying thermal operating conditions in an internal combustion engine. Temperature variations during engine warm-up are considered with oil rheology to observe texture-based improvements. Surface texture substantially reduces frictional energy loss during engine warm-up. Eight different monograde and multigrade engine oils are considered, and consistency is observed in texture-based improved outcomes.

**Keywords:** surface texture; journal bearing; friction; internal combustion engines

## 1. Introduction

Worldwide transportation of humans and goods consumes 20% of global primary energy; road vehicles account for 72% of this energy consumption [1]. Hydrodynamic friction-based energy losses are also particularly high during the engine warm-up period [2,3], especially at cold engine start-up because of high lubricant viscosities at low engine temperatures. Moreover, most vehicles operate at a temperature lower than the designed value because the length of intra-city journey is not sufficient to increase engine temperature to hot working conditions [4,5]. These conditions put a heavy burden on fuel economy and related environmental protection.

The performance of mating surfaces in an internal combustion (IC) engine is a major research concern because tribological interfaces cause energy losses. Recent studies suggest laser surface texture (LST) on relative surfaces as a potential option to reduce the hydrodynamic and boundary frictions [6]. These frictions are the main cause of energy losses in an engine, in particular, hydrodynamic friction at low temperatures during cold start-up and warm-up, and boundary friction at elevated engine temperatures. Mechanisms of friction reduction caused by surface textures include a small lubricating area, texture acting as an oil trap and micro-reservoir, and the micro-hydrodynamic effect [7]. Based on these mechanisms, surface texturing can be widely applied and benefit the mechanical seal, flat-faced tribo-pair, piston ring, thrust bearing, and journal bearing. The aforementioned adverse effects of

low engine temperatures were studied by few researchers, and energy losses were minimized with the use of surface textures [8]. However, such studies are rarely reported. Therefore, comprehensive optimization is needed to categorize surface textures for varying conformabilities of contact and operating conditions.

Most of the interfaces in an IC engine are non-elliptical contacts under sliding and/or reciprocating motions. Crankshaft bearings, piston ring–liner, piston skirt–liner, journal and thrust bearings, and cam–follower are some examples of such contacts. These machine components are widely used in numerous engineering applications aside from IC engines, thereby emphasizing the importance of understanding the effects of modern surfaces on the tribological performance of these contacts. Tribo-interfaces in an IC engine experience high-frequency fluctuating thermal and structural loads. Therefore, studies of such interfaces provide insight into the tribological performance of a wide-range of contacts in considerable applications.

A plain bearing is a crucial tribological component in IC engines; it contributes to increasing energy losses at cold temperatures [3]. Surface grooves in an interface improve the tribological performance in a number of engineering applications [9–12]. Therefore, this study numerically investigates the effect of grooves on the journal surface of big-end bearing in an IC engine during warm-up. In this study, transverse grooves are considered for modifying a journal–bearing interface. A 2D Reynolds equation is solved with realistic oil rheology at varying load and temperatures during the warm-up of an IC engine. The effects of hydrodynamic pressure, temperature, and shear rate on lubricant rheology are considered. Eight modern mono- and multigrade engine oils are used to draw a comprehensive conclusion. Texture-based tribological improvements are discussed in comparison with an untextured tribo-pair working under identical operating conditions.

## 2. Mathematical Model

The distribution ( $h$ ) of film thickness in a plain bearing interface with textures on the journal surface can be expressed as follows:

$$h(x, y) = (c(1 + \varepsilon \cos \theta) + h_t), \quad (1)$$

where  $x$  and  $y$  are the coordinates of a Cartesian coordinate system,  $\theta$  can be calculated by arctangent ( $y, x$ ) with two arguments,  $c$  is the difference between the radii of the bearing ( $R_B$ ) and the journal ( $R_J$ ),  $\varepsilon$  is the eccentricity ratio, and  $h_t$  is the film thickness based on surface textures.

Figure 1 represents the journal bearing hydrodynamic conjunction. Eccentricity ratio  $\varepsilon$  is used to reflect the effect of load, hence, hydrodynamic pressure ( $p$ ) is computed accordingly. Figure 2 illustrates the film thickness distribution over a partially textured journal surface compared with an untextured surface. Here, the axis of rotation is along the positive  $z$ -axis. As the perfectly aligned journal bearing is considered in the axial direction, a symmetric boundary condition is considered (as illustrated in Figure 2) at mid-plane of the bearing to reduce the computational domain to achieve a shortened computational time. Figure 3 illustrates the film thickness in the said mid-plane in a circumferential direction of textured and untextured journal–bearing interfaces.

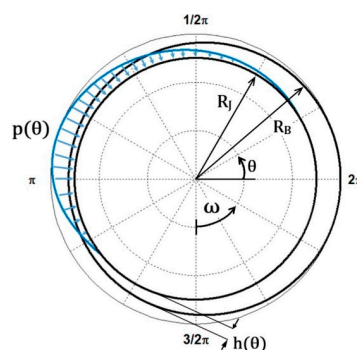
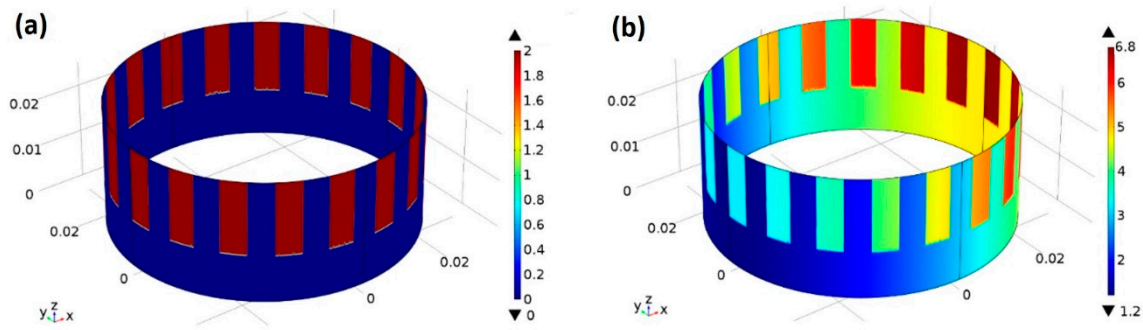
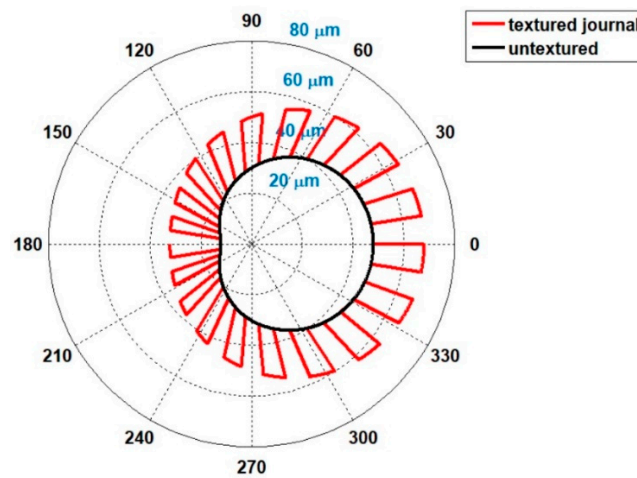


Figure 1. A journal bearing schematic illustration.



**Figure 2.** Oil film distributions over the journal bearing [ $10^{-5}$  m] are shown in Cartesian coordinates with the metric measuring units: (a) surface groove-dependent film ( $h_t$ ); (b) accumulative film thickness ( $c [1 + \varepsilon\cos\theta] + h_t$ ).



**Figure 3.** Lubricating oil film thickness at mid-plane of the textured and untextured journal surfaces.

The boundary separation between the oil film and the cavitation regions in the tribo-interfaces was made easy when Elrod [13] and Elrod and Adams [14] presented their work and algorithm. Based on their work, a modified Reynolds equation is used to compute hydrodynamic pressures in the journal–bearing interface in the present study. The equation is as follows:

$$\frac{\partial}{\partial x} \left[ \frac{\rho_c h^3 g \beta}{12\mu} \frac{\partial \Phi}{\partial x} \right] + \frac{\partial}{\partial y} \left[ \frac{\rho_c h^3 g \beta}{12\mu} \frac{\partial \Phi}{\partial y} \right] = \frac{1}{2} \frac{\partial}{\partial x} (\Phi \rho_c h u) + \frac{\partial}{\partial t} (\Phi \rho_c h), \quad (2)$$

where  $\rho_c$  is the density of cavitation region,  $\mu$  is the oil viscosity (Equation (7)),  $u$  is the sliding velocity of the journal surface,  $\beta$  is the bulk modulus of the typical lubricant oils and is  $10^9$  Pa [13], therefore, 1 GPa is the considered value in the present study,  $g$  is the switch function presented as follows:

$$g = \begin{cases} 0 & \text{if } 0 < \Phi < 1 \\ 1 & \text{if } \Phi \geq 1 \end{cases} \quad (3)$$

Uniform lubricant density is considered in the cavitation region; striated oil flow causes  $\Phi < 1$  because  $\Phi = \rho / \rho_c$ . Fluid film region results in  $\Phi > 1$  because  $\rho > \rho_c$ . The corresponding film pressure is:

$$p = p_c + \beta(\Phi - 1), \quad (4)$$

where  $p_c$  is the cavitation pressure, set at 50 kPa (absolute pressure) [15].

Bearings are subjected to dynamic structural and thermal loads in an IC engine. Variations in lubricant viscosity, calculated by the formulation presented in this study, at varying temperatures and pressures are shown in Figure 4. Using well-established models of lubricant rheology predicted the

depicted change under thermal and structural loads. Vogel [16] and Roelands–Houpert equations [17] and Cross [18] formulation were used to predict temperature, pressure, and shear rate-based changes in lubricant viscosity, respectively.

$$\mu_1 = \mu_0 e^{\frac{K_1}{(T-K_2)}} e^{[\ln(\mu_0)+9.67]\{(1+(1.51 \times 10^{-9})p)^Z-1\}}, \tag{5}$$

$$Z = \frac{1 \times 10^{-8}}{(5.1 \times 10^{-9})(\ln(\mu_0) + 9.67)} \tag{6}$$

where  $K_1$  and  $K_2$  are oil-dependent constants to match the temperature–viscosity behavior, and  $\mu_0$  is the viscosity atmospheric temperature. The pressure–viscosity coefficient used in Equation (5) considers the effect of variation of oils (Equation (6)) and is valid over the range of temperatures used in this study [17].

Figure 5 shows the effect of the operating conditions on the shear rates for an untextured journal surface. The Cross equation [18] is used to calculate shear-dependent viscosity, as follows:

$$\mu = \mu_2 + \frac{(\mu_1 - \mu_2)}{1 + m\dot{\gamma}^k} \tag{7}$$

where  $\mu_1$  is the limiting viscosity at zero shear rate,  $\mu_2$  is the limiting viscosity at high shear rate,  $m$  and  $k$  are fitting parameters and are considered to be 0.001 and 2/3, respectively, and  $\dot{\gamma} = |u|/h$  is the shear rate. Table 1 presents the oil parameters used in this study. Since the low shear rate viscosity ( $\mu_1$ ) varies with operating temperatures and pressure (Equation (5)), the ratio of high shear rate viscosity to low shear rate viscosity ( $\mu_2/\mu_1$ ) is used in to determine  $\mu_2$  accordingly. Multigrade oils are particularly subjected to pseudoplastic behavior [17], hence,  $\mu_2/\mu_1$  is considered equal to 1 for monograde oils, as reported in the following table.

Table 1. Oil parameters used in this study.

Oil	SAE							
	10	30	50	5W30	10W30	10W50	20W40	20W50
$\mu_2/\mu_1$	1.00	1.00	1.00	0.71	0.86	0.49	0.40	0.43

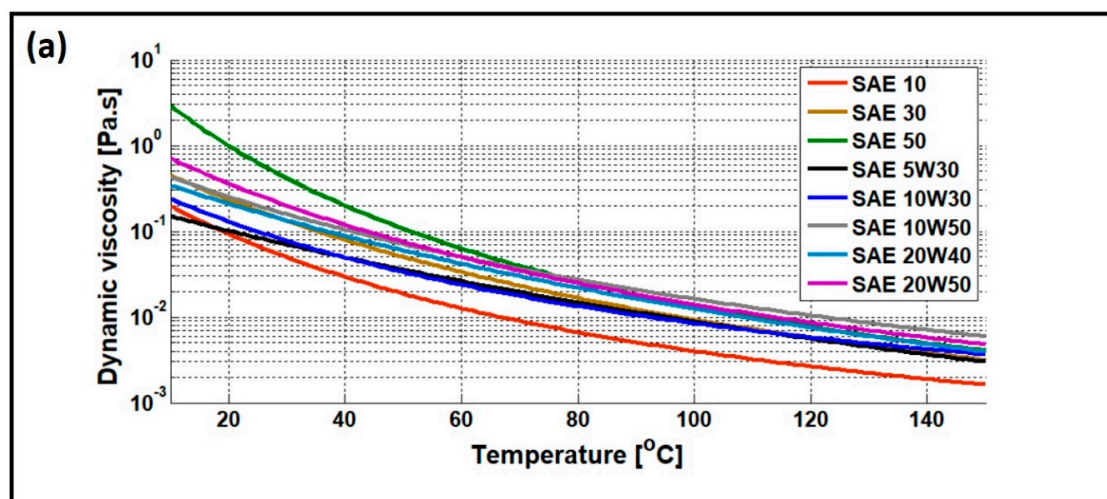


Figure 4. Cont.

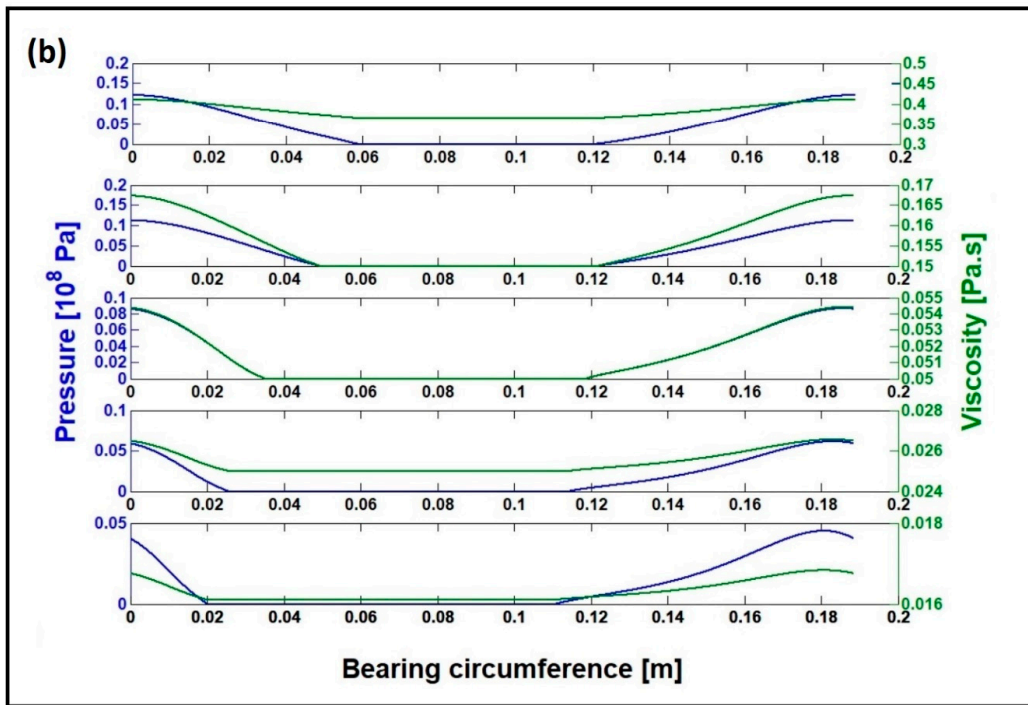


Figure 4. Viscosity dependency on: (a) temperature for used oils [19]; (b) hydrodynamic pressure for SAE 10W30.

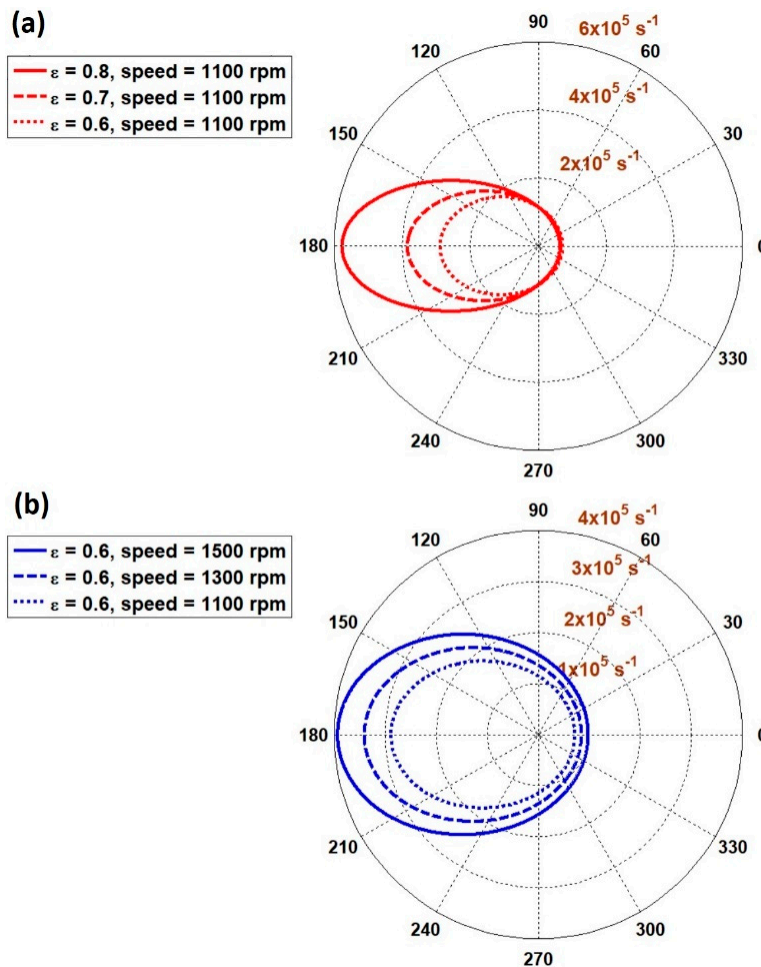


Figure 5. Variation in shear rate along the circumference of the bearing for varying: (a) loads; (b) speeds.

Available studies and optimization of surface texture results obtained by the authors of this study revealed that the area density ( $S_p$ ) and the aspect ratio ( $\epsilon$ ) are important parameters. These parameters are described mathematically as follows:

$$S_p = \frac{l_g \times w_g}{l_{cell} \times w_{cell}} \quad (8)$$

$$\epsilon = \frac{h_g}{w_g} \quad (9)$$

where  $h_g$  is the height of grooves,  $l_g$  and  $l_{cell}$  are the lengths of a groove and of the texture cell, respectively, and  $w_g$  and  $w_{cell}$  are the widths of the groove and of the cell. Figure 6 illustrates said geometric parameters in a schematic view.

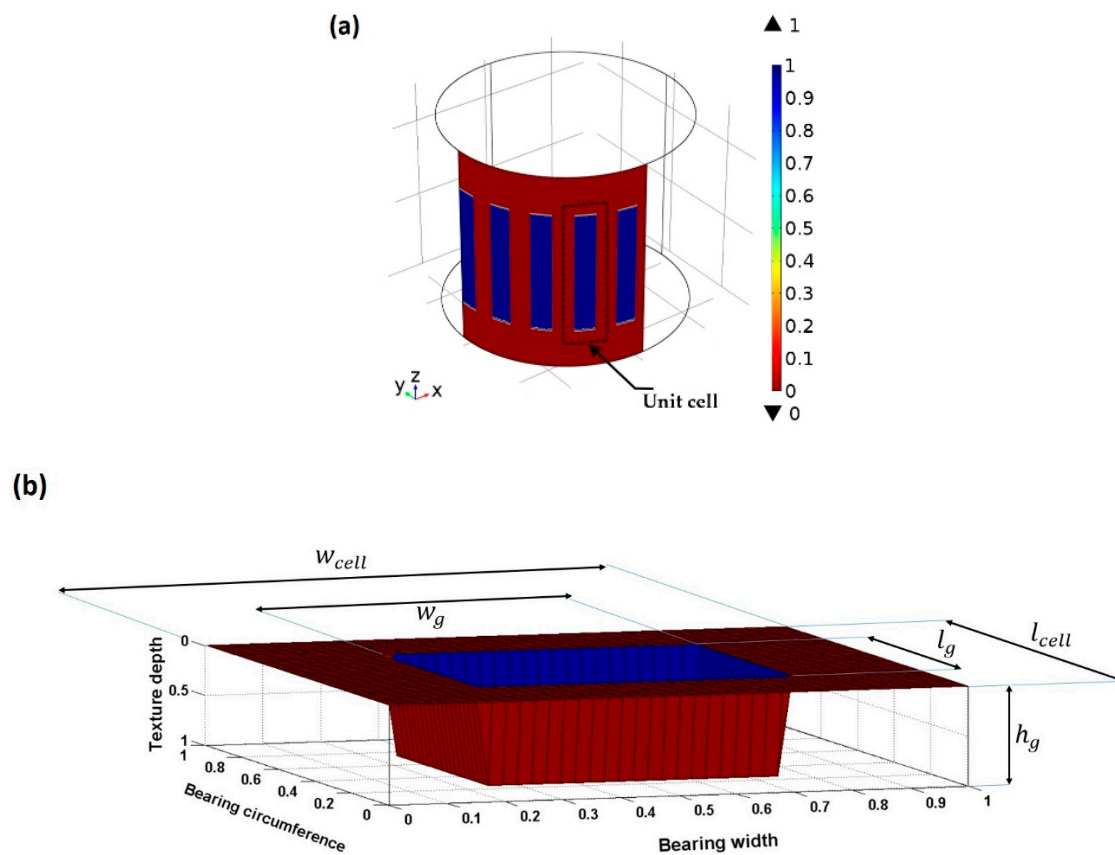


**Figure 6.** Geometric parameters of a texture in a cell over the journal surface: (a) unit cell representation of the journal surface with dimensionless texture depth; (b) parameter representation in a magnified view.

Based on the aforementioned studies on surface texturing, shallow dimples with a depth of  $20 \mu\text{m}$  and 19 grooves are considered on the journal surface. These values are considered after exhaustive optimization was performed by the authors for maximum friction reduction when load carrying capacity is affected to a minimum extent [20].

Journal bearings are designed to operate in the hydrodynamic regime of the lubrication. Oil film supports the applied load, and hydrodynamic pressure may be integrated over the journal surface to compute the load-carrying capacity of the interface [21]:

$$W_h = \int_0^w \int_0^{2\pi} p d\theta dz \quad (10)$$

where  $w$  is the width of the journal along the  $z$ -axis of the coordinate system.

Similarly, friction in this hydrodynamic interface can be computed by the following equation [17]:

$$F_{friction} = \int_0^{2\pi} \int_0^w \mu \frac{u}{h} \pm \frac{h}{2} \frac{\partial p}{\partial x} dA \quad (11)$$

Integrating the power loss over the time elapsed during the warm-up period of the engine (i.e.,  $\int_0^{t_{cycle}} F_{friction} \cdot R \cdot \omega dt$ ) can determine the energy consumed by the friction. Subsequently, energy saving owing to the texturing of the surfaces can be evaluated.

### 3. Numerical Procedure and Result Methodology

COMSOL Multiphysics (5.0, COMSOL Inc, Stockholm, Sweden) is a Finite Element Method-based commercial package used to solve the aforementioned mathematical model. A tolerance of  $10^{-3}$  is used in numerical iterations. Table 2 shows the vales of the parameters used in this study.

**Table 2.** Vales of geometric parameters used in this study.

Parameter	Value
Radius of the bearing	30 mm
Width of the bearing	50 mm
Minimum clearance	30 $\mu$ m
Groove depth	20 $\mu$ m
No. of grooves	19

The number of grooves and the corresponding depth are selected after performing exhaustive numerical simulations to achieve the optimum tribo-performance. Moreover, the outcomes of the mathematical model used in this study are compared, by the authors of the present work, with those related to lubricated sliding contacts already available in the literature (Figure 7). Negligible errors were found in the hydrodynamic lubricating regime used in this study. A mesh dependency (Figure 8) test was then performed to ensure the correctness of the results presented in this research work. The hydrodynamic pressure profile varies for varying mesh sizes. However, the difference in the spatial pressure values for two consecutive mesh sizes remains negligible (i.e., less than 2%). Therefore, keeping in view the safety factor to avoid any possible numerical diffusion and in order to save computational time, Mesh B is used in the present study.

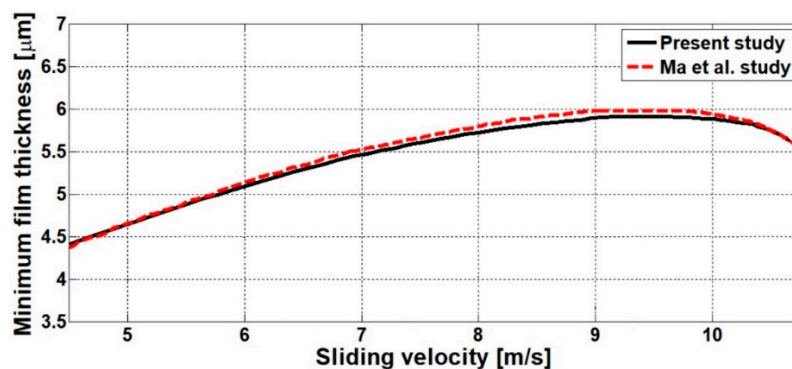


**Figure 7.** Validation of the mathematical model used in this study.

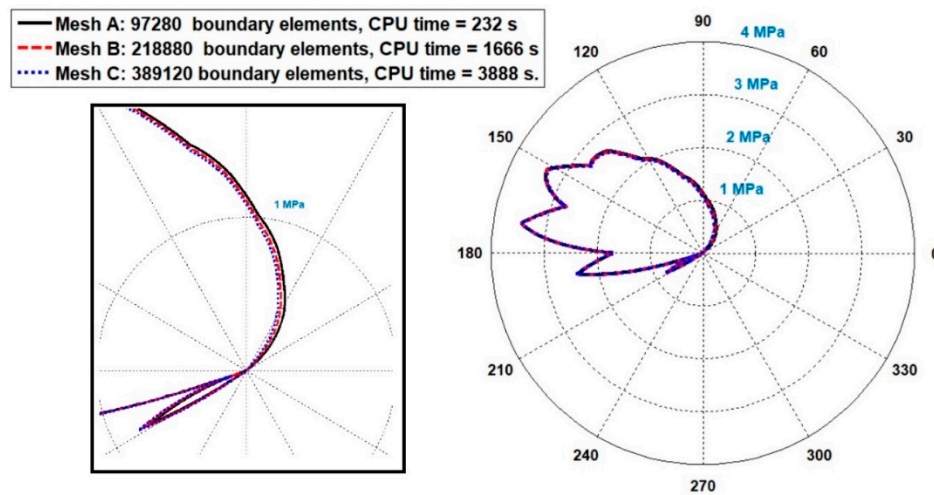


**Figure 8.** Hydrodynamic pressure variation for varying mesh sizes; mesh-dependency test. The left side of the figure presents a magnified view for a better appreciation of the difference shown in the right side of the figure.

A comparison is made for the tribological performance of textured and untextured journal bearings in the warm-up period (20 °C to 80 °C) of an IC engine crankcase temperature. This warm-up process of the engine was based on a time step corresponding to temperature changes of 20 °C to show the improvements caused by the surface textures. Unless stated otherwise, the results presented refer to SAE 10W30 engine oil.

#### 4. Results and Discussion

Figure 9 shows the friction torque caused by the hydrodynamic conjunction at the journal–bearing interface for a textured journal surface compared with plain bearing tribo-pairs without surface textures. The developing behavior of the friction torque is also illustrated over the entire warm-up period. Viscous friction was elevated at the cold start of the engine, due to high lubricant viscosity. The viscosities of engine oils decrease with increasing temperature, thereby reducing the friction torque. Textures cause a significant improvement in the frictional behavior of the interface for the time steps considered during warm-up of an IC engine.

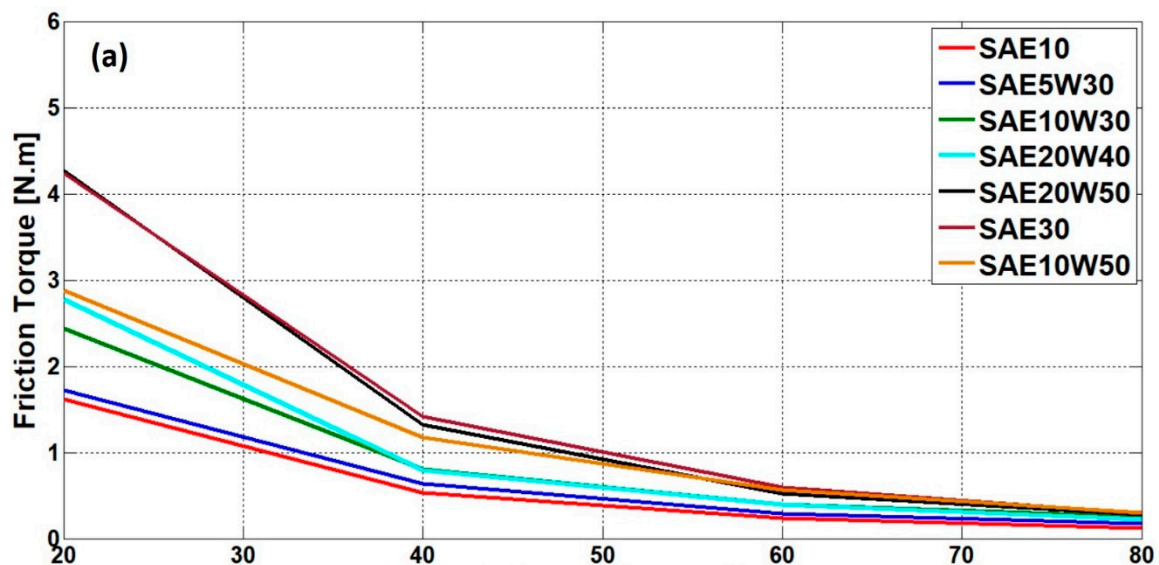


**Figure 9.** Cont.

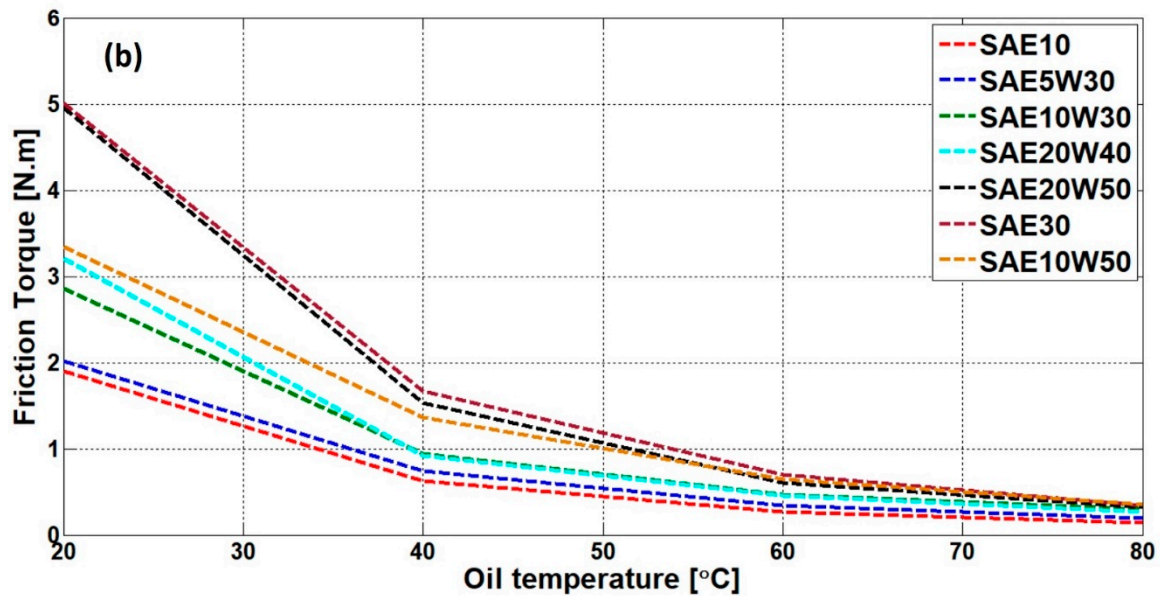


Figure 9. Hydrodynamic frictional torque in a (a) textured journal surface—bearing interface; (b) untextured journal bearing during the warm-up period of an IC engine.

This improved frictional response remains consistent for the monograde and multigrade oils considered in the study. Friction is higher at the same temperature for high viscous lubricant oils than for low viscous oils, such as SAE 10W30. Thus, lowly viscous lubricant oils are preferred in high-speed engines of domestic vehicles. However, the surface texture on the journal surface provides a similar quantity (%) of friction reduction for the engine oil considered in the study, as shown in Figure 10.

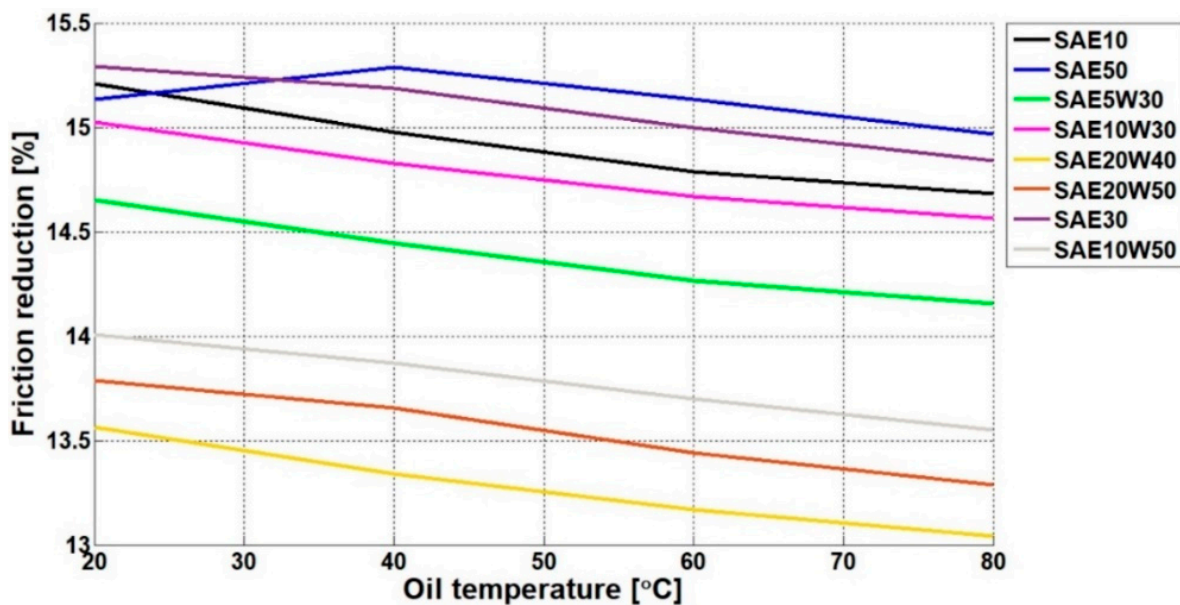
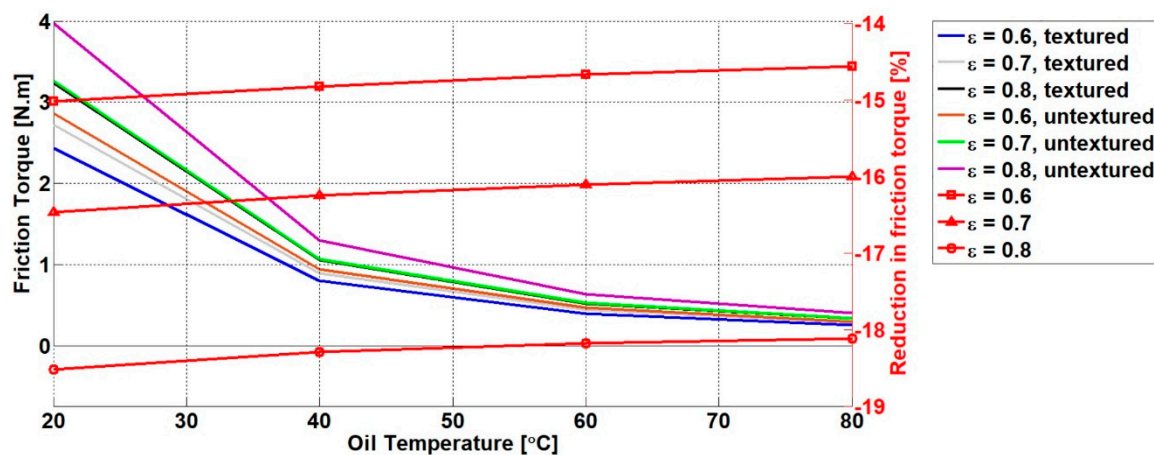


Figure 10. Surface texture-based friction reduction for the journal–bearing interface at varying temperatures of the IC engine for eight different multi- and monograde engine oils.

The mean reduction in the friction at cold start temperatures for eight different oils is 14.58% with a standard deviation of  $\pm 0.70\%$ . Similarly, the friction reduction for the considered oils is  $14.13 \pm 0.75\%$  at a warm engine temperature of 80 °C. Hence, textures on the journal surface provide nearly consistent friction reduction for varying lubricant oils and temperatures.

Figure 11 shows the journal bearing friction torque with textures on the journal surface compared with the untextured journal bearing for increasing load (i.e.,  $\epsilon$  ranging from 0.6 to 0.8) during the considered time steps to observe the developing behavior during an increase in temperature (20 °C to 80 °C). The results showing greater reduction of texture-based friction for increasing loads and oil temperatures are highly encouraging. Similar trends are observed in the percentage reduction of friction torque with increasing oil temperatures for different loads applied on the interface. Hence, the textured journal surface led to improved behaviors of a dynamically loaded journal bearing with transient loads.



**Figure 11.** Friction and reduction in the friction for textured and untextured journal bearings at varying loads during the warm-up process of an IC engine.

Pressure perturbation of the hydrodynamic interaction in the journal bearing reduces friction. Figure 12 shows the variations in the pressure profiles for increasing temperatures during the warm-up process. Metric measuring units are used in the coordinate system shown in the Figure 12. This micro-hydrodynamic effect is more visible at low temperatures than at high temperatures. This effect can also be observed for the mid-plane of the bearing in Figure 13. Moreover, the cavitation pattern also changes with the changing temperatures and lubricant oils. Figure 14 presents the fractional film content in a textured bearing. One multigrade (SAE 10W30) and two monograde (SAE 10 and SAE 30) oils are used to illustrate the change in frictional film content over the warm-up period. The developing effects of lubrication in the warm-up time are evident. Although the position of film reformation varies with increasing temperatures, the film rupture position substantially varies with increasing temperature. Surface textures also delay film reformation at the trailing edge compared with the untextured interface.

The aforementioned change in the pressure gradient in the circumferential direction with the reduced shear-based viscous friction reduce the total friction of the interface. The increased length of cavitation also contributes to the decrease of hydrodynamic friction. These effects substantially reduce friction. Energy consumed by textured and untextured journal bearings and energy saving caused by texturing of the surfaces during warm-up of an IC engine at varying speeds and loads are shown in Figures 15 and 16.

The energy saving trends for the oils (used in this study) remain consistent for a range of applied loads on the interface. However, energy saving caused by surface textures increases in an interface under high loads. Low-viscosity oils show a slightly better response to surface textures. Increase in energy loss at the interface also increases with increasing speed. By contrast, texture-based reduction in energy loss remains invariant with increasing engine warm-up speeds.

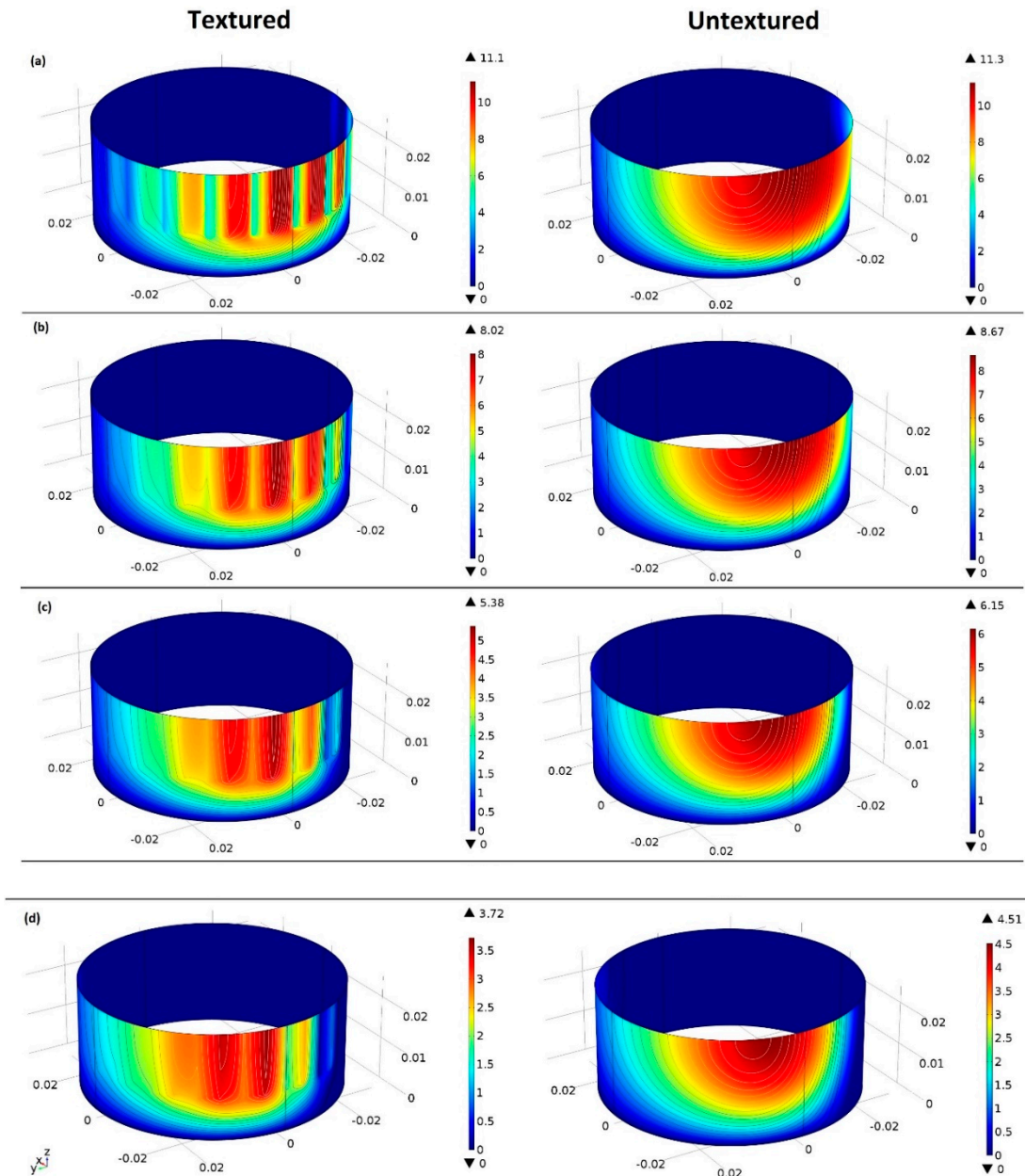


**Figure 12.** Hydrodynamic pressure (MPa) generation on textured journal bearing compared with the untextured journal bearing at: (a) 20 °C; (b) 40 °C; (c) 60 °C; (d) 80 °C.

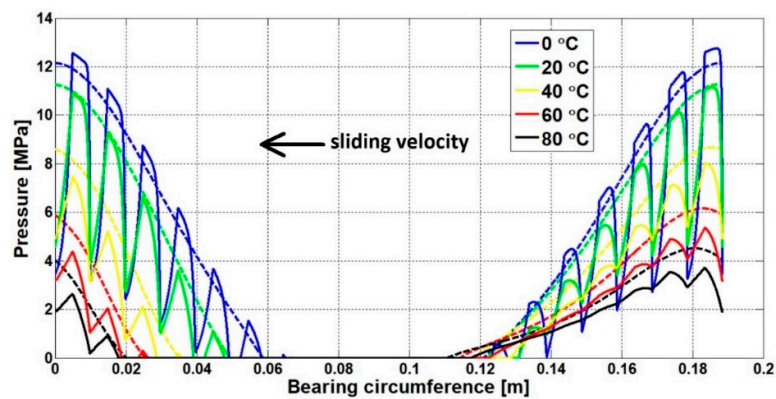


**Figure 13.** Hydrodynamic pressure and cavitation length variations for textured and untextured plain bearings at the crankshaft of an engine running at 1100 rpm in the warm-up period from 0 °C to 80 °C.

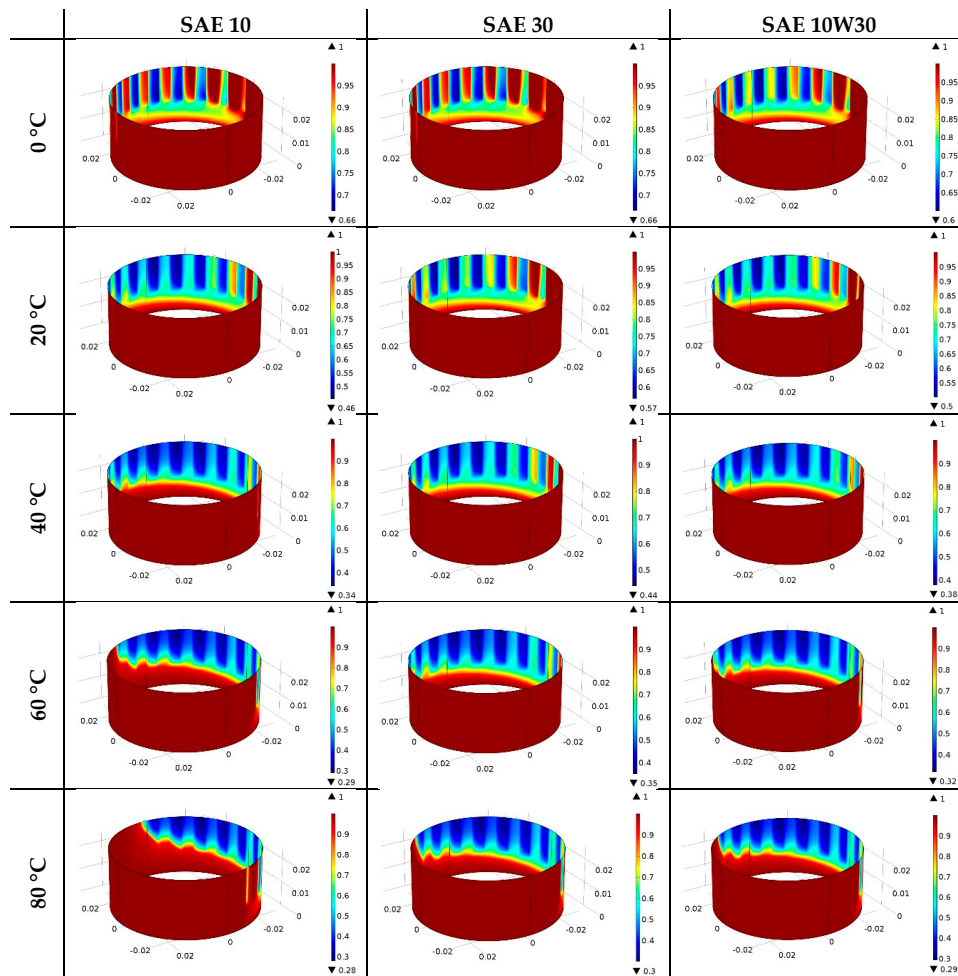


Figure 14. Fractional film content for monograde and multigrade oils at increasing temperatures during engine warm-up.

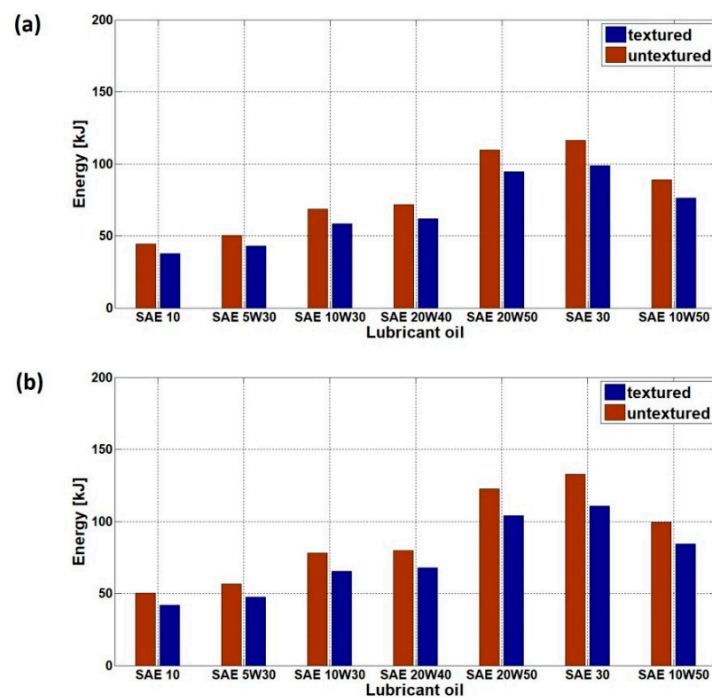


Figure 15. Cont.

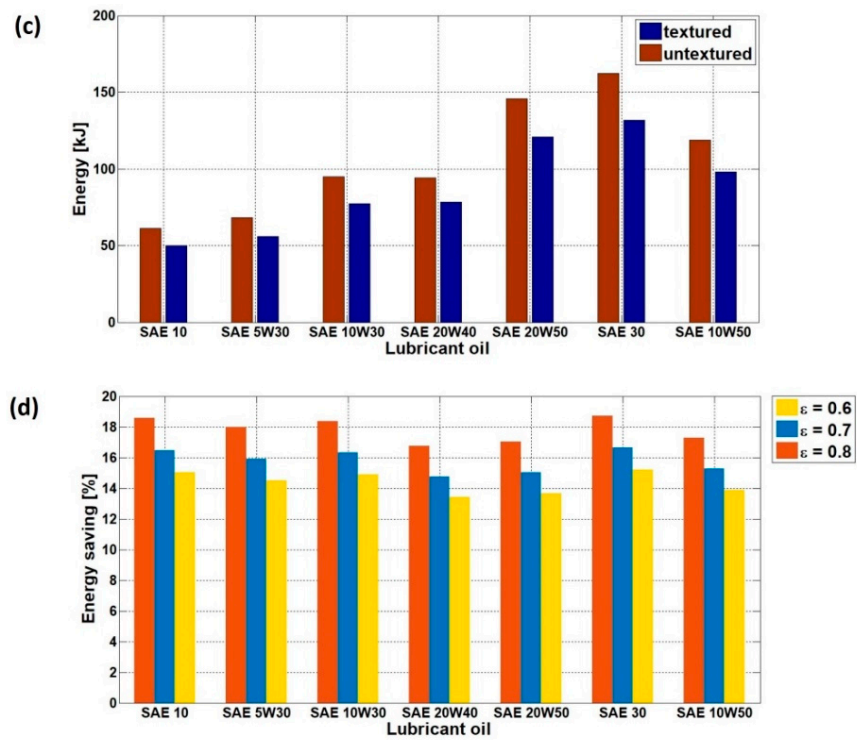


Figure 15. Comparison of fuel energy consumption during engine warm-up period of textured and untextured bearing surfaces at varying loads: (a)  $\epsilon = 0.6$ ; (b)  $\epsilon = 0.7$ ; (c)  $\epsilon = 0.8$ ; (d) percentage of energy saving produced by the surface textures.

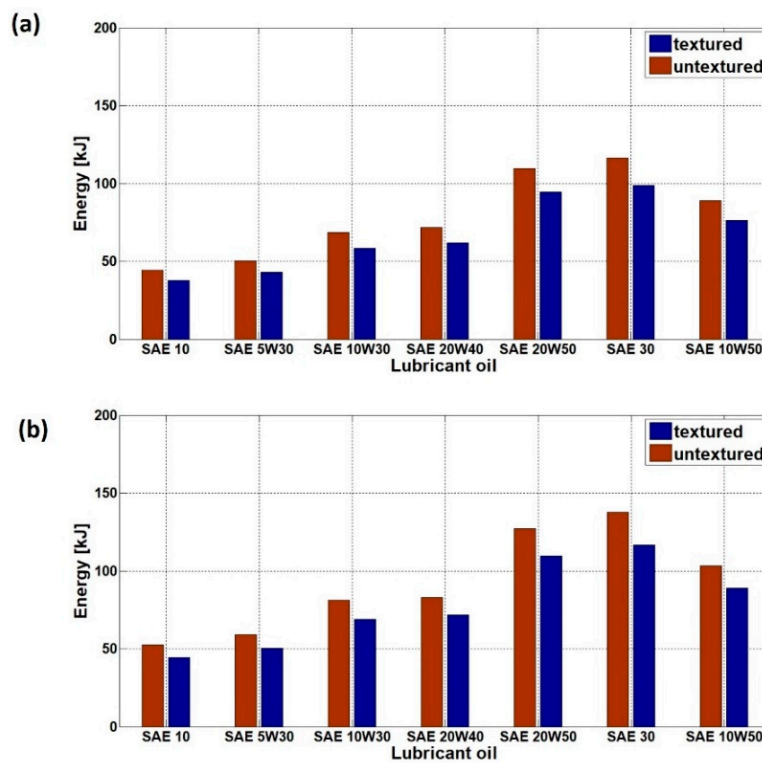
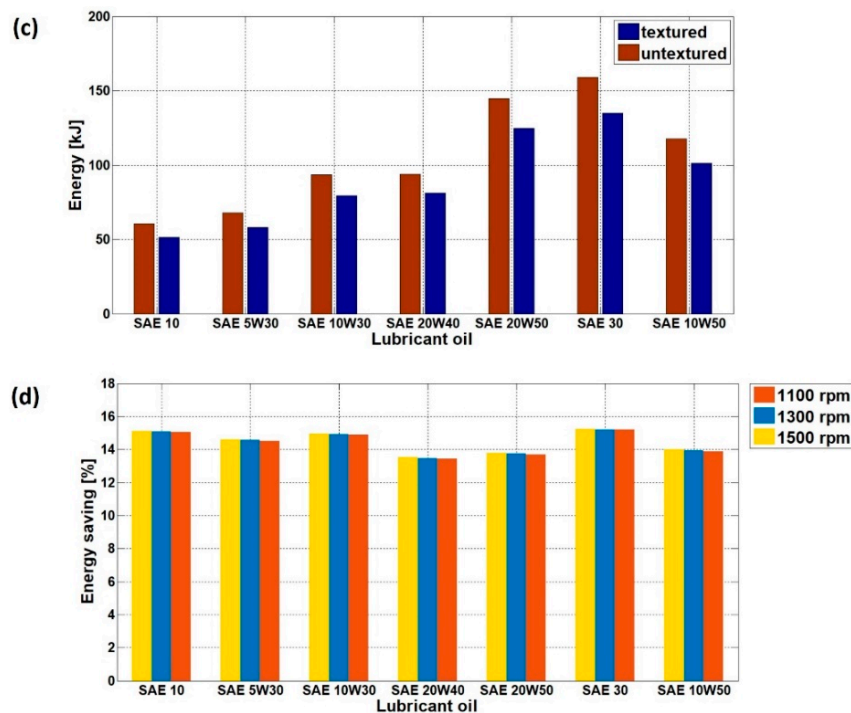


Figure 16. Cont.



**Figure 16.** Comparison of fuel energy consumption during the warm-up period of textured and untextured bearing surfaces at varying engine speeds: (a) 1100 rpm; (b) 1300 rpm; (c) 1500 rpm; (d) percentage of energy saving produced by the surface textures.

## 5. Conclusions

A numerical study was performed to predict the texture surface-based improved tribological performance of a journal bearing. Transverse grooves normal to the sliding direction were considered on the journal surface. Nineteen grooves with a shallow depth (texture depth  $\leq 20 \mu\text{m}$ ) were used to produce textures on the surface. The aforementioned geometric parameters of the textures were selected on the basis of previous studies performed by the authors of the present work. Temperature variations during the warm-up process of an IC engine were considered to observe the performance variations for varying thermal conditions. The performance of the textured journal surface was also evaluated for increasing loads on the interface. The frictional response of the interface substantially improved provided the said modifications were performed on the journal surface. Eight different engine oils were tested, and frictional improvements were found to be consistent. Moreover, nearly constant texture-dependent improved tribological performance was noted for the changing frictional behavior corresponding to increased engine temperatures. Surface texturing reduced the friction, and this reduction also increased with the applied load on the interface. Hence, grooves on the journal surface are a potential solution for reducing friction of an IC engine during the warm-up process and hot engine operations.

**Author Contributions:** All the authors of present study contributed equally in conducting and reporting this study.

**Funding:** A grant from the Priority Research Centers Program through the National Research Foundation of Korea (NRF) funded by the MEST (No. 2010-0020089) and an NRF grant funded by the Korean government (MSIP) (No. 2017R1A2B2005515) also supported this study.

**Acknowledgments:** The Higher Education Commission of Pakistan supported and provided financial support for this study. The Bio Experimental Fluid Engineering Laboratory of Kyungpook National University South Korea also provided technical assistance in performing this research.

**Conflicts of Interest:** The authors declare no conflicts of interest.

## References

1. Holmberg, K.; Andersson, P.; Erdemir, A. Global energy consumption due to friction in passenger cars. *Tribol. Int.* **2012**, *47*, 221–234. [[CrossRef](#)]
2. Roberts, A.; Brooks, R.; Shipway, P. Internal combustion engine cold-start efficiency: A review of the problem, causes and potential solutions. *Energy Convers. Manag.* **2014**, *82*, 327–350. [[CrossRef](#)]
3. Daniels, C.C.; Braun, M.J. The Friction Behavior of Individual Components of a Spark-Ignition Engine During Warm-Up. *Tribol. Trans.* **2006**, *49*, 166–173. [[CrossRef](#)]
4. Liu, Z.; Li, L.; Deng, B. Cold start characteristics at low temperatures based on the first firing cycle in an LPG engine. *Energy Convers. Manag.* **2007**, *48*, 395–404. [[CrossRef](#)]
5. Dato, A.N.G.; Fox, M.F. *An Initial Investigation of the Lubricant Condition in the Automotive Ring Zone under Cold Start Conditions*; Dowson, D., Priest, M., Dalmaz, G., Lubrecht, A.A., Eds.; Tribology Series; Elsevier: Amsterdam, The Netherlands, 2003; pp. 517–522.
6. Etsion, I. Modeling of surface texturing in hydrodynamic lubrication. *Friction* **2013**, *1*, 195–209. [[CrossRef](#)]
7. Imai, N.; Kato, T. Effects of texture patterns on hydrodynamic and mixed lubrication characteristics. *Proc. Inst. Mech. Eng. Part J J. Eng. Tribol.* **2013**, *227*, 898–904. [[CrossRef](#)]
8. Usman, A.; Park, C.W. Modeling and simulation of frictional energy loss in mixed lubrication of a textured piston compression ring during warm-up of spark ignition engine. *Int. J. Engine Res.* **2017**, *18*, 293–307. [[CrossRef](#)]
9. Aggarwal, S.; Pandey, R.K. Frictional and load-carrying behaviours of micro-textured sector shape pad thrust bearing incorporating the cavitation and thermal effects. *Lubr. Sci.* **2017**, *29*, 255–277. [[CrossRef](#)]
10. Sinanoğlu, C.; Nair, F.; Karamış, M.B. Effects of shaft surface texture on journal bearing pressure distribution. *J. Mater. Process. Technol.* **2005**, *168*, 344–353. [[CrossRef](#)]
11. Usman, A.; Park, C.W. Optimizing the tribological performance of textured piston ring–liner contact for reduced frictional losses in SI engine: Warm operating conditions. *Tribol. Int.* **2016**, *99*, 224–236. [[CrossRef](#)]
12. Vladescu, S.-C.; Olver, A.V.; Pegg, I.G.; Reddyhoff, T. The effects of surface texture in reciprocating contacts—An experimental study. *Tribol. Int.* **2015**, *82 Pt A*, 28–42. [[CrossRef](#)]
13. Elrod, H.G. A Cavitation Algorithm. *J. Lubr. Technol.* **1981**, *103*, 350–354. [[CrossRef](#)]
14. Elrod, H.; Adams, M. *A Computer Program for Cavitation and Starvation Problems*; Mechanical Engineering Publications: London, UK, 1976; pp. 37–41.
15. Chong, W.W.F.; Teodorescu, M.; Vaughan, N.D. Cavitation induced starvation for piston-ring/liner tribological conjunction. *Tribol. Int.* **2011**, *44*, 483–497. [[CrossRef](#)]
16. Vogel, H. The law of relation between the viscosity of liquids and the temperature. *Phys. Z.* **1921**, *22*, 645–646.
17. Stachowiak, G.W.; Batchelor, A.W. *Engineering Tribology*, 3rd ed.; Butterworth-Heinemann: Burlington, NJ, USA, 2006; ISBN 9780750678360.
18. Cross, M.M. Rheology of non-Newtonian fluids: A new flow equation for pseudoplastic systems. *J. Colloid Sci.* **1965**, *20*, 417–437. [[CrossRef](#)]
19. Pulkrabek, W.W. *Engineering Fundamentals of the Internal Combustion Engine*; Pearson Prentice Hall: Upper Saddle River, NJ, USA, 2004; ISBN 9780131405707.
20. Usman, A.; Park, C.W. Numerical optimization of surface texture for improved tribological performance of journal bearing at varying operating conditions. *Ind. Lubr. Tribol.* **2018**. [[CrossRef](#)]
21. Malik, S.; Kakoty, S.K. Analysis of dimple textured parallel and inclined slider bearing. *Proc. Inst. Mech. Eng. Part J J. Eng. Tribol.* **2014**, *228*, 1343–1357. [[CrossRef](#)]

